

## High Temperature X-Ray Study of the Thermal Expansion of PtS<sub>2</sub>, PtSe<sub>2</sub>, PtTe<sub>2</sub> and PdTe<sub>2</sub>

ARNE KJEKSHUS and FREDRIK GRØNVOLD

*Kjemisk Institutt A, Universitetet i Oslo, Blindern, Norway*

PtS<sub>2</sub>, PtSe<sub>2</sub>, PtTe<sub>2</sub> and PdTe<sub>2</sub>, all with structures of the Cd(OH)<sub>2</sub>-type and  $c/a < 1.633$ , have been studied by the X-ray powder method at temperatures in the range from 20 to 950°C. The thermal expansion is considerably anisotropic for all four compounds. For the  $a$ -axis it is almost linear over the whole temperature range, with linear thermal expansion coefficient,  $\beta_a$ , equal to  $2.3 \times 10^{-6} \text{ }^\circ\text{C}^{-1}$  for PtS<sub>2</sub> (20–562°C),  $5.7 \times 10^{-6} \text{ }^\circ\text{C}^{-1}$  for PtSe<sub>2</sub> (20–946°C),  $5.8 \times 10^{-6} \text{ }^\circ\text{C}^{-1}$  for PtTe<sub>2</sub> (20–870°C) and  $12.0 \times 10^{-6} \text{ }^\circ\text{C}^{-1}$  for PdTe<sub>2</sub> (20–574°C). For the  $c$ -axis the thermal expansion is approximately linear at lower temperatures only, and the expansion coefficient,  $\beta_c$ , equal to  $37 \times 10^{-6} \text{ }^\circ\text{C}^{-1}$  for PtS<sub>2</sub> (20–250°C),  $20 \times 10^{-6} \text{ }^\circ\text{C}^{-1}$  for PtSe<sub>2</sub> (20–283°C),  $27 \times 10^{-6} \text{ }^\circ\text{C}^{-1}$  for PtTe<sub>2</sub> (20–591°C) and  $30 \times 10^{-6} \text{ }^\circ\text{C}^{-1}$  for PdTe<sub>2</sub> (20–284°C). At higher temperatures the  $c$ -axis of PtS<sub>2</sub>, PtSe<sub>2</sub> and PtTe<sub>2</sub> increases more slowly than at lower temperatures, while the  $c$ -axis of PdTe<sub>2</sub> increases more rapidly. For all compounds the volume expansion has a temperature dependence similar to that of the  $c$ -axis. The average thermal volume expansion coefficient,  $\alpha$ , is  $40 \times 10^{-6} \text{ }^\circ\text{C}^{-1}$  for PtS<sub>2</sub> (20–250°C),  $31 \times 10^{-6} \text{ }^\circ\text{C}^{-1}$  for PtSe<sub>2</sub> (20–283°C),  $39 \times 10^{-6} \text{ }^\circ\text{C}^{-1}$  for PtTe<sub>2</sub> (20–591°C) and  $57 \times 10^{-6} \text{ }^\circ\text{C}^{-1}$  for PdTe<sub>2</sub> (20–284°C). The interatomic distances between metal and metalloid atoms, and between the metalloid atoms, have been calculated for the various temperatures.

Although detailed investigations are necessary for a complete description of the thermal movement of the atoms or molecules forming a crystal, some information might, in simple cases, be obtained from the thermal expansion of the crystal. Because of anharmonic vibrations in the crystals the expansion is generally not isotropic<sup>1</sup>. For layer structures the anisotropic expansion in favor of the direction normal to the layers is explainable on the basis of weak bonds between the atoms in different layers.

The present paper concerns the thermal expansion of PtS<sub>2</sub>, PtSe<sub>2</sub> and PtTe<sub>2</sub><sup>2</sup> and PdTe<sub>2</sub><sup>3</sup>, all of which have structures of the Cd(OH)<sub>2</sub>-type. A drawing of four unit cells of the Cd(OH)<sub>2</sub>-type structure is shown in Fig. 1. Filled circles represent metal atoms in (0 0 0), while open circles represent metalloid atoms

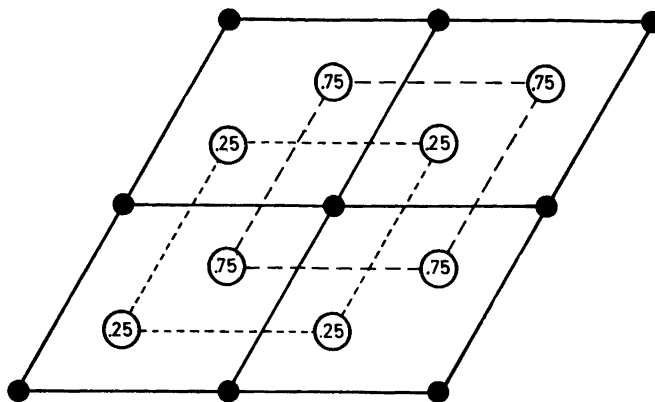


Fig. 1. Projection of four unit cells of the  $\text{Cd}(\text{OH})_2$ -type structure on (001).

in  $(\frac{2}{3} \frac{1}{3} z)$  and  $(\frac{1}{3} \frac{2}{3} \bar{z})$ , with  $z = 0.250$ . From Fig. 1 it is seen that both metal and metalloid atoms form hexagonal nets, but at different heights. In the projection they are repeated at every  $1/3$  face diagonal.

Only a few compounds with this type of structure have been examined at temperatures other than room temperature. Megaw<sup>4</sup> studied the thermal expansion of single crystals of  $\text{Ca}(\text{OH})_2$  and  $\text{Mg}(\text{OH})_2$  by X-ray methods from 0 to  $100^\circ\text{C}$ . For these compounds the coefficient of expansion normal to the hexagonal layers was found to be 3 to 4 times larger than parallel to the layers.

Bredig<sup>5</sup> examined  $\text{CdI}_2$ , which forms polytypic structures based upon the  $\text{Cd}(\text{OH})_2$ -structure<sup>6</sup>, and found that this compound also exhibits relatively large thermal expansion normal to the hexagonal layers. (From 25 to  $325^\circ\text{C}$   $\beta_c$  is approximately  $4 \times 10^{-5} \text{ }^\circ\text{C}^{-1}$ , while  $\beta_a$  is  $1 \times 10^{-5} \text{ }^\circ\text{C}^{-1}$ ).

$\text{NiTe}_2$ , with  $\text{Cd}(\text{OH})_2$ -type structure, has been studied at several temperatures up to  $800^\circ\text{C}$  by Schneider and Imhagen<sup>7</sup>. They also determined the lattice constants of different samples in the composition range from  $\text{NiTe}$  ( $\text{NiAs}$ -type structure) to  $\text{NiTe}_2$  as function of temperature.

Other compounds with layer structures, *e.g.* graphite<sup>8</sup>, and boron nitride<sup>9</sup>, show contraction in the hexagonal layers with increasing temperature, and large expansion perpendicular to the layers.

## EXPERIMENTAL

The platinum chalcogenides were prepared from stoichiometric amounts of the elements heated in evacuated, sealed silica tubes at  $825^\circ\text{C}$  and slowly cooled to room temperature. The palladium ditelluride was prepared at  $600^\circ\text{C}$ .

Information about the purity of the elements is given elsewhere<sup>2,3</sup>.

X-Ray powder photographs of the compounds were taken in a 190 mm Unicam high-temperature camera, with the samples sealed in thin-walled quartz capillaries. The samples were studied at temperatures between 20 and  $950^\circ\text{C}$ .  $\text{PtS}_2$  and  $\text{PdTe}_2$  could not, however, be examined at the very highest temperatures,  $\text{PtS}_2$  because of its great dissociation pressure<sup>10</sup> which made the thin-walled quartz capillaries burst, and  $\text{PdTe}_2$  because of its relatively low melting point of about  $700^\circ\text{C}$ .

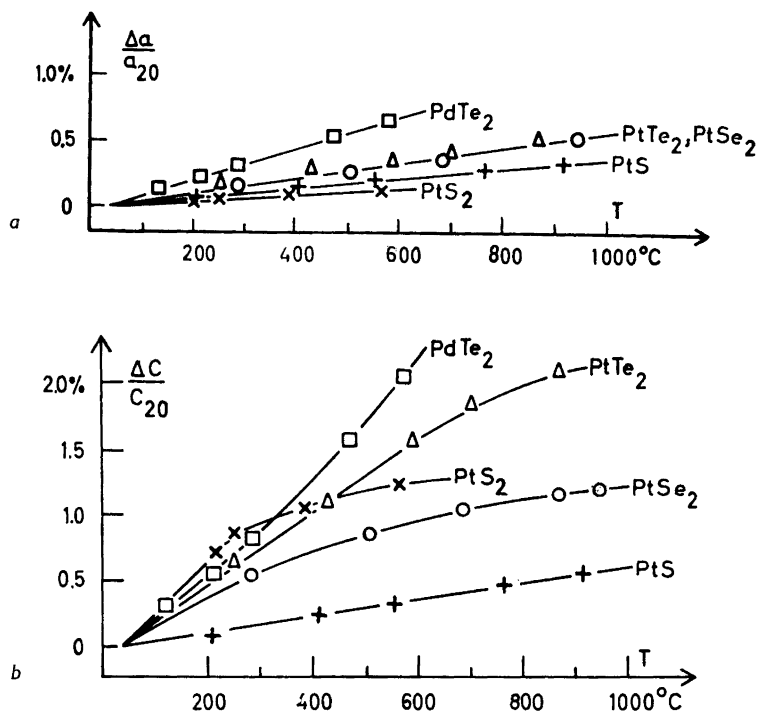
By means of a voltage regulator, the registered temperature of the furnace surrounding the specimen was kept constant within  $\pm 5^\circ\text{C}$ . The Pt/Pt-Rh thermocouples of the furnace had been calibrated with a standard couple located at the position of the specimen. Lattice constants are given in Ångström units ( $\lambda\text{CuK}\alpha_1 = 1.54050 \text{ \AA}$ ). Only the high-angle reflections of the diffraction pattern were used in the calculation of the lattice constants. The probable error in the lattice constant determinations at temperatures above room temperature is estimated to be about 0.02 %. This includes a possible error due to variation in the composition of the sample with temperature.

## RESULTS

The results of the lattice constant measurements are listed in Table 1. Here is also listed the  $c/a$  ratio, the unit cell volumes, the shortest interatomic distances between metal and metalloid atoms [ $(000)(2/3 \ 1/3 \ 0.250)$ ] and between the metalloid atoms [ $(2/3 \ 1/3 \ 0.250)$  ( $1/3 \ 2/3 \ 0.250$ )]. For every measured or

Table 1. Lattice constants, unit cell volumes and interatomic distances for  $\text{PtS}_2$ ,  $\text{PtSe}_2$ ,  $\text{PtTe}_2$  and  $\text{PdTe}_2$  at different temperatures.

Sample	$T(^{\circ}\text{C})$	$a(\text{Å})$	$c(\text{Å})$	$c/a$	$V(\text{Å}^3)$	Metal-metalloid distance (Å)	Metalloid-metalloid distance (Å)
$\text{PtS}_2$	20	3.5431	5.0389	1.422	54.782	2.402	3.245
	215	3.5442	5.0745	1.432	55.203	2.408	3.260
	250	3.5449	5.0822	1.434	55.309	2.409	3.261
	385	3.5463	5.0911	1.436	55.449	2.411	3.267
	562	3.5474	5.1000	1.438	55.580	2.413	3.271
$\text{PtSe}_2$	20	3.7278	5.0813	1.363	61.152	2.499	3.330
	283	3.7337	5.1089	1.368	61.679	2.506	3.343
	503	3.7377	5.1235	1.371	61.988	2.510	3.350
	683	3.7420	5.1325	1.372	62.240	2.513	3.355
	865	3.7463	5.1384	1.372	62.455	2.516	3.358
946	3.7482	5.1405	1.372	62.544	2.517	3.360	
$\text{PtTe}_2$	20	4.0259	5.2209	1.297	73.283	2.666	3.495
	256	4.0326	5.2531	1.303	73.981	2.673	3.510
	431	4.0357	5.2777	1.308	74.442	2.678	3.520
	591	4.0386	5.3026	1.313	74.900	2.682	3.531
	707	4.0419	5.3152	1.315	75.201	2.685	3.537
870	4.0452	5.3279	1.317	75.504	2.689	3.543	
$\text{PdTe}_2$	20	4.0365	5.1262	1.270	72.333	2.660	3.464
	120	4.0420	5.1422	1.272	72.757	2.664	3.472
	210	4.0446	5.1538	1.274	73.015	2.667	3.478
	284	4.0495	5.1685	1.276	73.401	2.671	3.485
	470	4.0577	5.2061	1.283	74.233	2.680	3.502
	574	4.0632	5.2303	1.287	74.782	2.686	3.513



Figs. 2a, b. Relative lattice constant variations as function of temperature.

calculated property  $x_T$ , the ratio  $\frac{x_T - x_{20}}{x_{20}} = \frac{\Delta x}{x_{20}}$  is calculated and plotted as  $\frac{\Delta x}{x_{20}}$  versus  $T$ . The calculations of the expansion coefficients were based upon these data.

The change in length of the cell edges with temperature is rather different along the different axes. As shown in Fig. 2a, the  $a$ -axis of all four compounds increases linearly with increasing temperature. The expansion coefficient  $\beta_a$  is equal to  $2.3 \times 10^{-6} \text{ }^\circ\text{C}^{-1}$  for PtS<sub>2</sub> (20–562°C),  $5.7 \times 10^{-6} \text{ }^\circ\text{C}^{-1}$  for PtSe<sub>2</sub> (20–946°C),  $5.8 \times 10^{-6} \text{ }^\circ\text{C}^{-1}$  for PtTe<sub>2</sub> (20–870°C) and  $12.0 \times 10^{-6} \text{ }^\circ\text{C}^{-1}$  for PdTe<sub>2</sub> (20–574°C). The corresponding curves for the  $c$ -axis are shown in Fig. 2b. Those for PtS<sub>2</sub>, PtSe<sub>2</sub> and PtTe<sub>2</sub> are of similar shape, while that for PdTe<sub>2</sub> is different. At lower temperatures the thermal expansion of the  $c$ -axis is linear, with expansion coefficient  $\beta_c$  equal to  $37 \times 10^{-6} \text{ }^\circ\text{C}^{-1}$  for PtS<sub>2</sub> (20–250°C),  $20 \times 10^{-6} \text{ }^\circ\text{C}^{-1}$  for PtSe<sub>2</sub> (20–283°C),  $27 \times 10^{-6} \text{ }^\circ\text{C}^{-1}$  for PtTe<sub>2</sub> (20–591°C) and  $30 \times 10^{-6} \text{ }^\circ\text{C}^{-1}$  for PdTe<sub>2</sub> (20–284°C). At higher temperatures the  $c$ -axis of PtS<sub>2</sub>, PtSe<sub>2</sub> and PtTe<sub>2</sub> increases more slowly than at lower temperatures. The curve for the  $c$ -axis of PdTe<sub>2</sub> has the opposite curvature, and rises more sharply than at lower temperatures. In the temperature region just

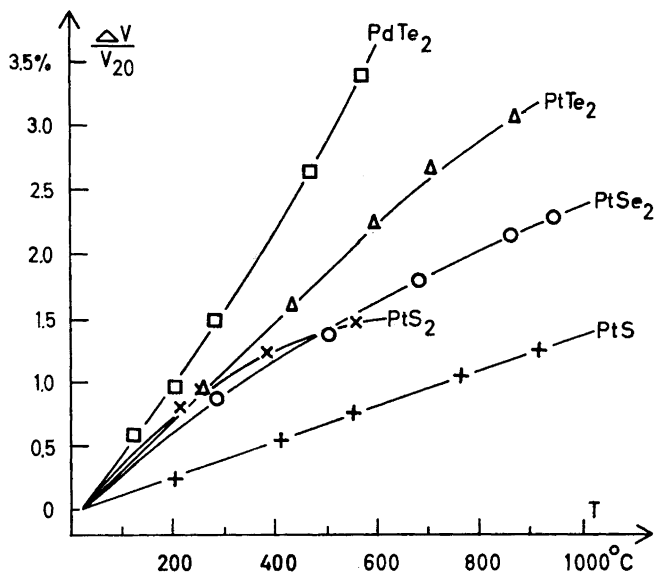


Fig. 3. Relative volume expansions as function of temperature.

below melting a fairly large increase in the coefficient of thermal expansion for the  $c$ -axis of  $\text{PdTe}_2$  seems to occur.

The volume expansion is plotted as function of temperature in Fig. 3. For all compounds the volume expansion has a similar temperature dependence as the  $c$ -axis. The first part of the curves is approximately linear. The average thermal volume expansion coefficient  $\alpha$  is  $40 \times 10^{-6} \text{ }^\circ\text{C}^{-1}$  for  $\text{PtS}_2$  (20–250°C),  $31 \times 10^{-6} \text{ }^\circ\text{C}^{-1}$  for  $\text{PtSe}_2$  (20–283°C),  $39 \times 10^{-6} \text{ }^\circ\text{C}^{-1}$  for  $\text{PtTe}_2$  (20–591°C) and  $57 \times 10^{-6} \text{ }^\circ\text{C}^{-1}$  for  $\text{PdTe}_2$  (20–284°C).

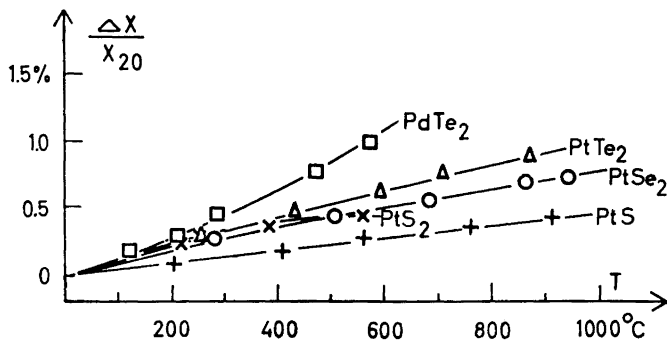


Fig. 4. Relative changes in interatomic bond distance between metal and metalloid atoms with temperature.

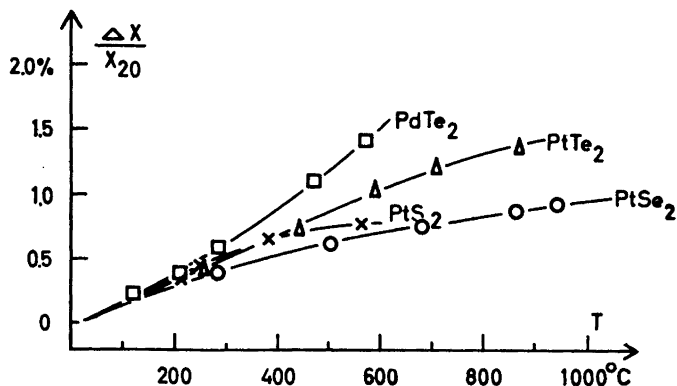


Fig. 5. Relative changes in the shortest metalloid-metalloid distance with temperature.

As seen from Fig. 4, the changes in bond distance are of the same order of magnitude as the average linear expansion. The expansion curves have a linear region with expansion coefficients  $11 \times 10^{-6} \text{ }^\circ\text{C}^{-1}$  for  $\text{PtS}_2$  (20–250°C),  $10 \times 10^{-6} \text{ }^\circ\text{C}^{-1}$  for  $\text{PtSe}_2$  (20–283°C),  $11 \times 10^{-6} \text{ }^\circ\text{C}^{-1}$  for  $\text{PtTe}_2$  (20–591°C), and  $16 \times 10^{-6} \text{ }^\circ\text{C}^{-1}$  for  $\text{PdTe}_2$  (20–284°C). The shortest metalloid-metalloid distances (*cf.* Fig. 5) change similarly, while the shortest metal-metal distances vary as the *a*-axis. The expansion coefficient over the linear region in Fig. 5 is  $17 \times 10^{-6} \text{ }^\circ\text{C}^{-1}$  for  $\text{PtS}_2$  (20–250°C),  $15 \times 10^{-6} \text{ }^\circ\text{C}^{-1}$  for  $\text{PtSe}_2$  (20–283°C),  $17 \times 10^{-6} \text{ }^\circ\text{C}^{-1}$  for  $\text{PtTe}_2$  (20–591°C), and  $23 \times 10^{-6} \text{ }^\circ\text{C}^{-1}$  for  $\text{PdTe}_2$  (20–284°C). The changes in the metal-metalloid and the metalloid-metalloid distances are calculated on the assumption that the parameter *z* has the same value  $z = 0.250$  at all temperatures.

#### DISCUSSION

The present results show agreement with the expansion measurements<sup>4</sup> of  $\text{Mg}(\text{OH})_2$  and  $\text{Ca}(\text{OH})_2$  with regard to linearity and strong anisotropy of the expansion coefficients in the lower temperature range. The measurements were, however, only carried to about 100°C and deviations from linearity of the expansion coefficient might well take place at higher temperatures. From the results of Schneider and Imhagen<sup>7</sup> on  $\text{NiTe}_2$  the curvature of the lattice constant variation could not be obtained with certainty.

Comparison with results from thermal expansion of compounds with other than  $\text{Cd}(\text{OH})_2$ -type structures will here be limited to compounds with supposedly similar chemical bond type. Results for  $\text{MnTe}$ <sup>11</sup> and  $\text{CrSb}$ <sup>12</sup>, both with NiAs-type structure, are similar in the temperature range below the antiferromagnetic transition temperature to those found for  $\text{PdTe}_2$ . In the range from –100 to +50°C the thermal expansion coefficient of the *a*-axis of  $\text{MnTe}$  is almost zero, while for the *c*-axis it increases with temperature. In the range from 0 to 450°C the *a*-axis of  $\text{CrSb}$  increases linearly, while the *c*-axis increases more rapidly than at lower temperatures.  $\text{FeS}$  and  $\text{FeS}_{1.09}$  also with NiAs-like

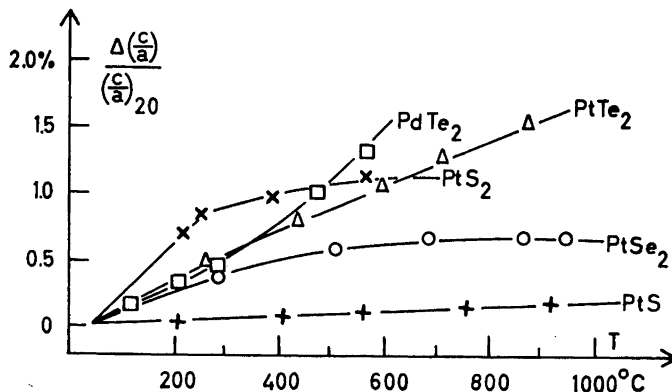


Fig. 6. Relative changes in the  $c/a$  ratio with temperature.

structures have been examined<sup>13</sup> in the temperature range from 20 to 385°C. Both  $a$ -axis and  $c$ -axis are found to increase with temperature. The expansion in the hexagonal plane is larger than perpendicular to it. For FeS  $\beta_a \approx 1.5 \times 10^{-5} \text{ }^\circ\text{C}^{-1}$ ,  $\beta_c \approx 0$  (20–138°C) and  $\beta_a \approx 1.7 \times 10^{-4} \text{ }^\circ\text{C}^{-1}$ ,  $\beta_c \approx 4 \times 10^{-5} \text{ }^\circ\text{C}^{-1}$  (138–325°C), and for FeS<sub>1.09</sub>  $\beta_a \approx 5 \times 10^{-5} \text{ }^\circ\text{C}^{-1}$ ,  $\beta_c \approx 8 \times 10^{-6} \text{ }^\circ\text{C}^{-1}$  (75–325°C).

The present authors have examined the thermal expansion of PtS with B17-type structure. This compound has linear expansion both in the  $a$ - and  $c$ -directions, with  $\beta_a \approx 3.9 \times 10^{-6} \text{ }^\circ\text{C}^{-1}$  (20–915°C) and  $\beta_c \approx 5.8 \times 10^{-6} \text{ }^\circ\text{C}^{-1}$  (20–915°C) (*cf.* Figs. 2a, b). As apparent from Fig. 6 the expansion is approximately isotropic. The volume expansion (*cf.* Fig. 3) is linear with coefficient ( $\alpha$ )  $13.7 \times 10^{-6} \text{ }^\circ\text{C}^{-1}$  in the temperature range studied. The platinum-sulfur bond distance shows a linear change in the examined temperature range with expansion coefficient  $4.7 \times 10^{-6} \text{ }^\circ\text{C}^{-1}$ , (*cf.* Fig. 4). The shortest metal-metal distance is also here equal to the length of the  $a$ -axis and shows the same variation with temperature (*cf.* Fig. 2a). There are two different short sulfur-sulfur distances which have the same relative variation as the  $a$ -axis and  $c$ -axis, respectively (*cf.* Figs. 2a, b).

Starting from absolute zero, the first part of a thermal expansion curve should be of sigmoidal type similar to the heat capacity curve. The reasons for the increase in volume at higher temperatures are not fully explained by the existing theories for the perfect lattice. On approaching melting, the curve is expected to show a rapid increase caused by an increasing number of lattice defects<sup>14</sup>. Fletcher<sup>15</sup> has attempted to show that the theories might account for the enhanced expansion without assuming lattice defects.

Of the compounds studied here only PdTe<sub>2</sub> shows an increase of the relative volume expansion at higher temperatures. This compound also has the lowest melting point. The relative expansions of PtS<sub>2</sub>, PtSe<sub>2</sub> and PtTe<sub>2</sub> are still on the upper part of the sigmoidal curve.

Fajans<sup>16</sup> has found that in chemical compounds there is usually an increase in the thermal expansion with decreasing electronegativity difference between the elements. This rule applies to the two compounds PtSe<sub>2</sub> and PtTe<sub>2</sub> with  $\alpha$  equal to  $31 \times 10^{-6} \text{ }^\circ\text{C}^{-1}$  and  $39 \times 10^{-6} \text{ }^\circ\text{C}^{-1}$ , respectively, but not to PtS<sub>2</sub> and PtSe<sub>2</sub> or PtTe<sub>2</sub> since the expansion coefficient of PtS<sub>2</sub>,  $40 \times 10^{-6} \text{ }^\circ\text{C}^{-1}$ , is greater than for the two others. The possibility that this might have been caused by PtS<sub>2</sub> losing sulfur due to dissociation at higher temperatures cannot be excluded. If one, however, considers the *a*-axes, the expansion coefficient  $\beta_a$  increases from the sulfide to the telluride.

*Acknowledgement.* The authors wish to thank Professor Haakon Haraldsen for his interest in this study and for placing laboratory facilities at their disposal.

#### REFERENCES

1. Grüneisen, E. and Goens, E. *Z. Physik* **29** (1924) 141.
2. Grønvold, F., Haraldsen, H. and Kjekshus, A. *To be published*.
3. Grønvold, F. and Røst, E. *Acta Chem. Scand.* **10** (1956) 1620.
4. Megaw, Helen D. *Proc. Roy. Soc. (London)* **142** (1933) 198.
5. Bredig, M. A. *J. Chem. Phys.* **24** (1956) 1037.
6. Mitchell, R. S. *Z. Krist.* **108** (1956) 296, 341.
7. Schneider, A. and Imhagen, K. H. *Naturwiss.* **44** (1957) 324.
8. Nelson, B. and Riley, D. P. *Proc. Phys. Soc. (London)* **57** (1945) 477.
9. Pease, R. S. *Acta Cryst.* **5** (1952) 356.
10. Biltz, W. and Juza, R. *Z. anorg. u. allgem. Chem.* **190** (1930) 161; see also Richardson, F. D. and Jeffes, J. H. F. *J. Iron Steel Inst. (London)* **171** (1952) 165.
11. Greenwald, Selma *Acta Cryst.* **6** (1953) 396.
12. Snow, A. I. *Revs. Modern Phys.* **25** (1953) 127.
13. Haraldsen, H. *Z. anorg. u. allgem. Chem.* **246**. (1941) 195.
14. Lawson, A. W. *Phys. Rev.* **78** (1950) 185.
15. Fletcher, C. C. *Phil. Mag.* **2** (1957) 639.
16. Fajans, K. *Phys. Rev.* **61** (1942) 543.

Received June 21, 1959.